Developmental Cell, Vol. 5, 99–111, July, 2003, Copyright ©2003 by Cell Press

The Ran GTPase Regulates Kinetochore Function

Alexei Arnaoutov and Mary Dasso*
Laboratory of Gene Regulation and Development
NICHD
NIH
Building 18, Room 106
Bethesda, Maryland 20892

Summary

The Ran GTPase is required for nuclear assembly, nuclear transport, spindle assembly, and mitotic regulation. While the first three processes are relatively well understood, details of Ran's role in mitotic progression remain obscure. We have found that elevated levels of Ran's exchange factor (RCC1) abrogate the spindle assembly checkpoint in *Xenopus* egg extracts, restore APC/C activity, and disrupt the kinetochore localization of checkpoint regulators, including Mad2, CENP-E, Bub1, and Bub3. Depletion of Ran's GTPase activating protein (RanGAP1) and its accessory factor (RanBP1) similarly abrogates checkpoint arrest. By contrast, the addition of RanGAP1 and RanBP1 to extracts with exogenous RCC1 restores the spindle checkpoint. Together, these observations suggest that the spindle checkpoint is directly responsive to Ran-GTP levels. Finally, we observe a clear wave of RCC1 association to mitotic chromosomes at the metaphase-anaphase transition in normal cycling extracts, suggesting that this mechanism has an important role in unperturbed cell cycles.

Introduction

Ran is a small GTPase required for nucleocytoplasmic trafficking, spindle assembly, nuclear assembly, and cell cycle control (Dasso, 2002). The nucleotide exchange factor for Ran, RCC1, is a chromatin-associated protein (Macara, 2001). The GTPase activating protein for Ran, RanGAP1, is cytoplasmic during interphase (Macara, 2001). During mitosis, the bulk of RanGAP1 is broadly distributed, although a significant fraction of RanGAP1 becomes associated with kinetochores (Joseph et al., 2002). Ran-GTP nucleotide hydrolysis requires a family of accessory proteins. The best-characterized member of this family is mammalian RanBP1, which is distributed to the cytosol during interphase. RanBP1 accelerates the rate of RanGAP1-mediated Ran-GTP hydrolysis by about an order of magnitude in vitro (Bischoff et al., 1995). RanBP1 also promotes dissociation of Ran-GTP from transport receptors, whose binding would otherwise block RanGAP-mediated GTP hydrolysis (reviewed in Macara, 2001). The distribution of Ran's regulators has been widely hypothesized to modulate local concentrations of Ran-GTP within the cell, spatially directing the many processes in which Ran has been implicated (Dasso, 2002).

*Correspondence: mdasso@helix.nih.gov

Ran's primary known effectors are a set of Ran-GTP binding proteins that were originally described as nuclear transport receptors. Ran-GTP binding regulates association between these proteins and their transport cargoes (Macara, 2001). During mitosis, the Importin β import receptor acts with its heterodimeric partner, Importin α, to bind and inhibit factors required for spindle assembly (Dasso, 2002). Targets of this inhibition include the mitotic spindle proteins TPX2 and NuMA. A locally high concentration of Ran-GTP generated by RCC1 may release inhibition by Importin β near chromosomes, and thereby facilitate bipolar spindle formation (Kalab et al., 2002).

Defects in the Ran pathway disrupt both the onset and the completion of mitosis (reviewed in Sazer and Dasso, 2000), although Ran's function in cell cycle progression has never been clearly distinguished from its roles in nuclear transport and spindle assembly. We were therefore interested in examining Ran's role in mitotic regulation more closely. Mitosis is tightly controlled in eukaryotes by the activity of Cyclin B and Securin (Peters, 2002). Both Cyclin B and Securin are ubiquitinated at the metaphase-anaphase transition by an E3 ligase called the anaphase-promoting complex/cyclosome (APC/C), working in association with its activators Cdc20/FZY and Cdh1/FZR (Peters, 2002). In the presence of misassembled spindles, with kinetochores that are unattached or that lack tension from spindle microtubules, the onset of anaphase is delayed through activation of a spindle assembly checkpoint. This checkpoint pathway prevents APC/C^{FZY} activation and thereby stabilizes APC/C^{FZY} substrates. After all of the chromosomes have become attached and aligned within the mitotic spindle, the checkpoint is turned off, APC/C^{FZY} becomes active, and anaphase commences (Musacchio and Hardwick, 2002; Peters, 2002). Components of the spindle assembly checkpoint include: Mad1, Mad2, Mps1, Bub1, Bub3, BubR1, and CENP-E (Abrieu et al., 2000; Chen et al., 1996; Sharp-Baker and Chen, 2001).

We have examined the role of Ran in regulating mitotic checkpoints using *Xenopus* egg extracts, a well-established model system for checkpoint control (Chen and Murray, 1997). During normal cell cycles in cycling egg extracts, we find that the amount of chromatin-associated RCC1 increases dramatically at the onset of Cyclin B destruction. Moreover, moderate levels of exogenous RCC1 protein abrogate mitotic spindle checkpoint arrest and allow Cyclin B destruction in extracts containing nuclei plus nocodazole. We find that the spindle assembly checkpoint in *Xenopus* is characterized by decreased APC^{FZY} activity, and addition of RCC1 to extracts with the activated checkpoint restores APC^{FZY} activity to control levels. In order to determine the precise mechanism through which RCC1 abrogates checkpoint arrest, we examined the localization of mitotic regulators, including Mad2, CENP-E, Bub1, and Bub3. We find that these proteins are mislocalized away from kinetochores in nocodazole-treated extracts after the addition of high levels of RCC1 protein. The displacement of checkpoint proteins from kinetochores did not

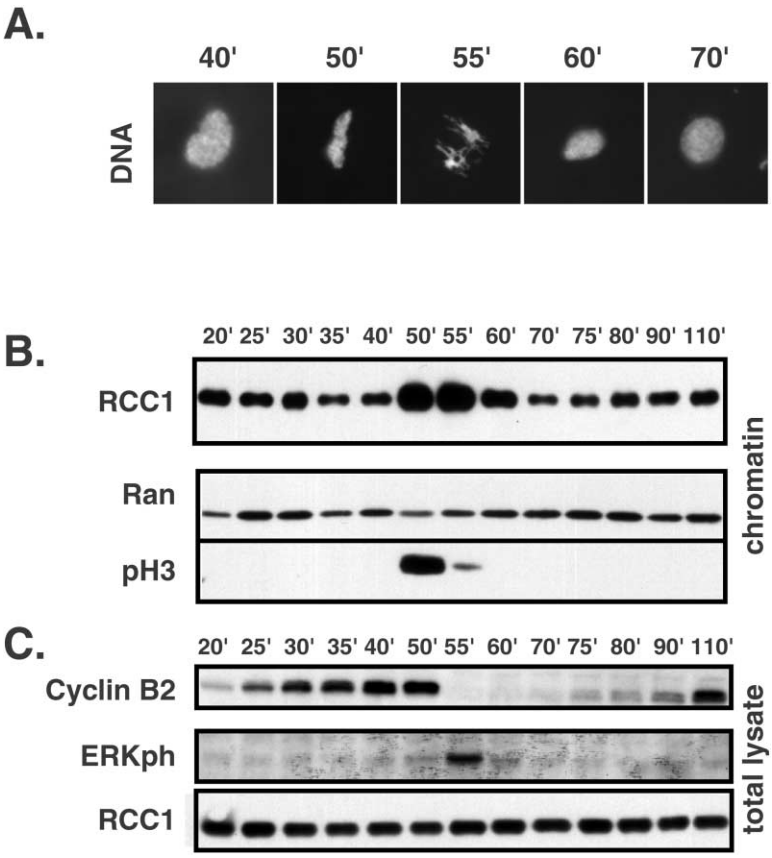

Figure 1. The Level of RCC1 on Chromatin Fluctuates during the Cell Cycle

Cycling extracts were supplemented with 2,000 nuclei per μl and incubated at 24°C.

(A) Aliquots were removed at the indicated times and analyzed for DNA morphology after addition of Hoechst 33258 DNA dye.

(B) Chromatin was purified from extracts at the indicated times and analyzed by SDS-PAGE for the abundance of RCC1, Ran, and phosphorylated histone H3.

(C) Extract samples taken at the indicated times were probed for the presence of Cyclin B2, phosphorylated ERK, and RCC1 by Western blotting.

require the Importin β protein. Interestingly, displacement of Bub1 and Bub3 from kinetochores could be reversed by the addition of recombinant RanGAP1 protein, suggesting that their behavior responds directly to Ran-GTP levels. Localization of Mad2 and CENP-E were not restored by RanGAP1, indicating either that their dissociation from kinetochores is not a simple result of elevated Ran-GTP levels, or that their sensitivity to Ran-GTP is more pronounced than Bub1 and Bub3.

Results

The Dynamics of RCC1 Association with Chromatin during the Cell Cycle

In *Xenopus* egg extracts, microtubule dynamics and spindle assembly are dependent upon the concentration of Ran-GTP (reviewed in Dasso, 2002). This finding has led to the hypothesis that chromatin-associated RCC1 protein creates an increased local concentration of Ran-GTP in the vicinity of chromosomes, helping to direct the formation of bipolar spindles. Because the chromosomal localization of RCC1 is central to this hypothesis, we examined whether RCC1 cofractionates with chromosomes throughout the embryonic cell cycle using *Xenopus* cycling extracts (Murray, 1991). To examine the behavior of RCC1 in this system, we made a crude chromosome-containing fraction by centrifugation to separate free RCC1 from RCC1 bound to large structures, such as nuclei or condensed chromosomes. We were surprised to find that the amount of RCC1 bound to chromatin changed significantly during the cell cycle (Figure 1). Remarkably, the level of RCC1 increased after nuclear envelope breakdown and peaked at the metaphase-to-anaphase transition, returning to its basal level when nuclear envelope formation was complete. These observations suggest that RCC1 interacts with chromatin in a cell cycle-dependent manner.

RCC1 Regulates the Spindle Assembly Checkpoint

It was notable that the highest levels of chromatin-associated RCC1 correlated closely with the mitotic phosphorylation of histone H3 and the onset of Cyclin B destruction (Figure 1). To investigate the role of RCC1/chromatin complexes during mitosis, we added recombinant RCC1 to extracts prepared from eggs arrested in second meiotic metaphase (CSF extracts). The addition of calcium to CSF extracts causes them to exit from meiotic arrest and enter mitotic cell cycles. However, if high concentrations of sperm nuclei and nocodazole are added to the extracts prior to calcium, the extracts will not exit from M phase because the spindle assembly checkpoint will be active and will prevent the degradation of APC/C targets (Chen and Murray, 1997).

Strikingly, elevation of RCC1 concentration by 10-fold over endogenous levels allowed CSF extracts with sperm nuclei and nocodazole to bypass checkpoint arrest and degrade both Cyclin B and Securin after calcium addition (Figure 2A). Nuclear envelopes also formed in the RCC1-treated extracts after calcium addition, providing morphological confirmation that they had progressed to interphase despite the presence of unattached kinetochores. The decreased size of nuclei assembled in extracts containing exogenous RCC1 would

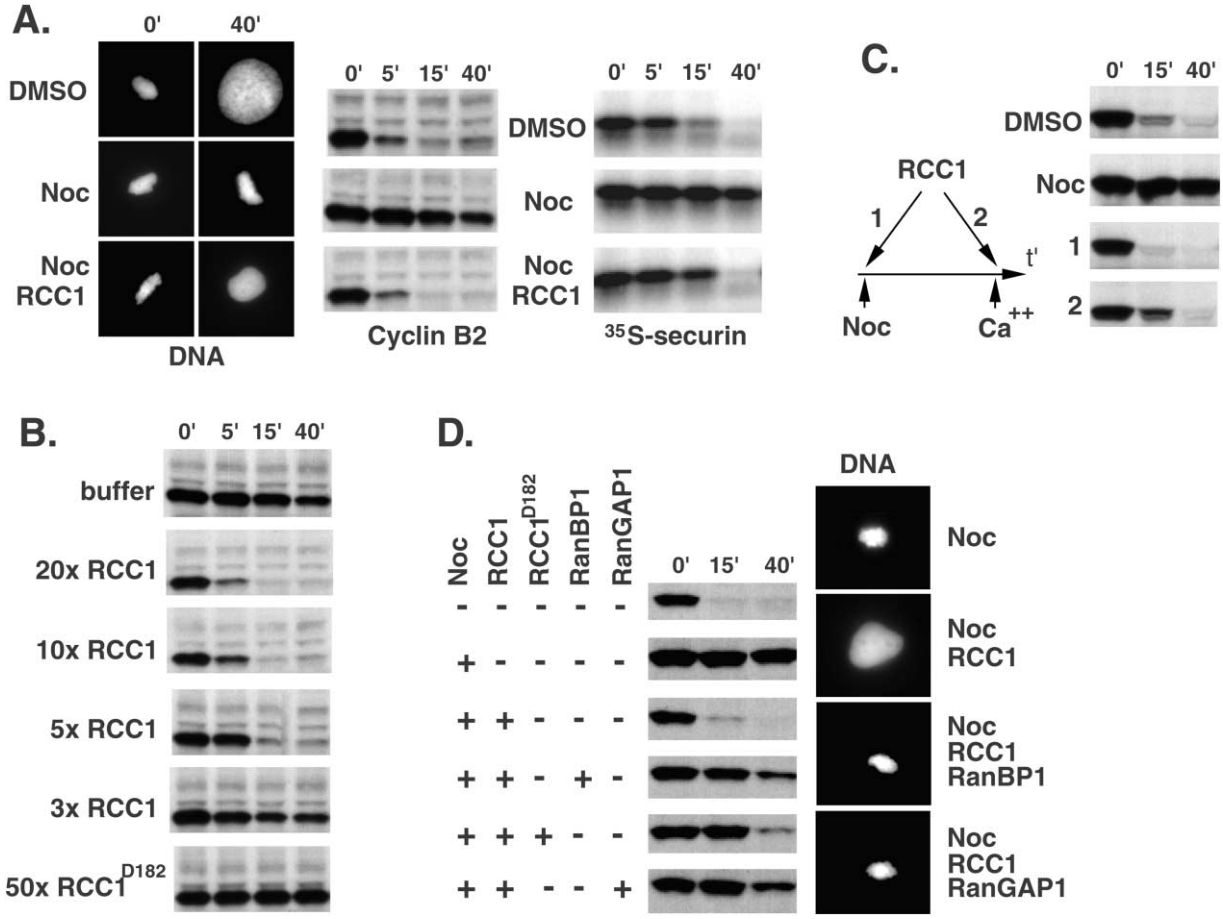

Figure 2. RCC1 Inactivates the Spindle Checkpoint

(A) CSF extracts with nuclei were treated with DMSO (upper panels), nocodazole (middle panels), or nocodazole plus 2.5 μM recombinant RCC1 (lower panels). After incubation for 45 min, extracts were stimulated with 0.6 mM Ca^{2+} to destroy CSF. At the indicated times after calcium addition, Hoechst 33258 dye was added for the examination of DNA morphology, and aliquots were removed for Western blot analysis with anti-Cyclin B2 antibodies. ^{35}S-labeled Securin was added to the same extracts at t = 0, aliquots were removed, processed for SDS-PAGE, and autoradiographed.

(B) CSF extracts with nuclei and nocodazole were treated with 3-, 5-, 10-, or 20-fold excess of wild-type RCC1 over endogenous (0.25 μM) or with 13 μM $RCC1^{D182}$. At the times indicated after Ca^{2+} addition, Cyclin B2 abundance was analyzed as in (A).

(C) Extracts were treated as above, except that RCC1 was added either 40 min prior to or together with Ca^{2+}. At the indicated times after calcium addition, Cyclin B2 abundance was analyzed as in (A).

(D) Extracts were treated as in (A), but 1.25 μM of RanGAP1 (endogenous: 0.25 μM) or 8 μM of His_6RanBP1 (endogenous: 0.8 μM) or 12.5 μM of $RCC1^{D182}$ was added simultaneously with 2.5 μM of RCC1, as indicated. After Ca^{2+} addition, Cyclin B2 abundance was analyzed as in (A).

be anticipated from previous results showing that nuclear transport and nuclear assembly are impaired by disturbance of the Ran pathway (Pu and Dasso, 1997). Addition of rhodamine-labeled tubulin showed that the bypass of the checkpoint was not due to the restoration of spindle assembly (data not shown). Moreover, there was no indication that exogenous RCC1 altered the stability of Cyclin B during CSF arrest prior to calcium addition or altered calcium-driven Cyclin B2 degradation in the absence of microtubule-disrupting drugs (Figure 2A, compare first lanes in each panel; data not shown). We also did not observe changes in chromosome morphology due to the addition of RCC1 prior to calcium release.

Taken together, these observations suggest that elevated levels of RCC1 can abrogate spindle checkpoint arrest in *Xenopus* egg extracts without restoring spindle assembly. This would imply that RCC1 interacts with and inactivates the checkpoint machinery.

RCC1 Disrupts the Spindle Checkpoint in a Dose-Dependent Manner

We analyzed the stability of checkpoint arrest with varying levels of exogenously added RCC1, increasing the total RCC1 concentration by 3- to 20-fold over endogenous levels. In these experiments, we assayed checkpoint arrest through Cyclin B abundance on Western blots (Figure 2B). We observed that the checkpoint was inactivated in a graded fashion: at low concentrations of added RCC1 (equivalent to 3-fold over endogenous), checkpoint arrest was maintained although a portion of Cyclin B was degraded. At moderate concentrations (5-fold), the checkpoint was not maintained, but the onset of Cyclin B degradation was slightly delayed compared to samples containing high levels of RCC1 (20-fold). Notably, an inactive mutant of RCC1 ($RCC1^{D182}$) did not inactivate the spindle assembly checkpoint, even when added at much higher levels than the wild-type RCC1 protein (50-fold). To the contrary, we observed

that RCC1^{D182} reproducibly promoted Cyclin B stability in extracts where the spindle assembly checkpoint was only partially active (data not shown).

To distinguish whether RCC1 disrupted the establishment or the maintenance of the checkpoint, we examined whether the timing of RCC1 addition was important for its capacity to override checkpoint arrest. We added RCC1 to nocodazole-treated CSF extracts either 45 min prior to or simultaneously with calcium (Figure 2C). In the latter case, we expected that the checkpoint signal would have been established before the addition of RCC1, such that RCC1 should have no effect if it exclusively disrupts the initiation of the checkpoint signal. As before, the sample preincubated with RCC1 from the start of the reaction exited mitosis promptly upon the addition of calcium. The sample to which calcium and RCC1 were added simultaneously also exited mitosis, albeit with a small, reproducible delay. These findings suggest that RCC1 is not only able to disrupt activation of the checkpoint signal pathway, but also capable of inactivating checkpoint arrest after it has been established.

We examined whether exogenous RCC1 disrupted checkpoint signaling by altering the balance of Ran-GTP versus Ran-GDP or by some other means. To address this question, we prepared recombinant human RanGAP1 and a tagged version of RanBP1 (His_6-S-RanBP1), the RanGAP1 accessory protein (Bischoff et al., 1995; Haberland and Gerke, 1999). We added RCC1 (10-fold endogenous) to a CSF extract containing sperm nuclei and nocodazole 45 min prior to calcium activation of mitotic exit. Immediately thereafter, we added either RanGAP1 (5-fold endogenous) or RanBP1 (10-fold endogenous) to aliquots of this reaction. Whereas the reaction containing only RCC1 degraded Cyclin B and exited from CSF arrest upon calcium addition as expected, the reactions that also contained either RanGAP1 or RanBP1 did not degrade Cyclin B efficiently and remained in mitosis (Figure 2D). This observation indicates that increased levels of the Ran-GTP hydrolysis induced by added RanGAP1 or RanBP1 can compensate for the increased nucleotide exchange activity from exogenous RCC1 and thus restore checkpoint signaling. We therefore conclude that mitotic checkpoint arrest can be eliminated by an increased GTP binding status of Ran.

Ran-GTP Regulates Spindle Checkpoint Activity and APC/C^{FZY} Inhibition

To understand the mechanism whereby exogenous RCC1 abrogates spindle checkpoint arrest in egg extracts, we wished to determine the molecular targets of RCC1's action in the checkpoint pathway. Current understanding of the spindle checkpoint suggests that kinetochores that are unattached or improperly attached produce an inhibitory signal that restrains APC/C^{FZY} activity, thereby preventing the onset of anaphase and sister chromatid separation (Musacchio and Hardwick, 2002). We measured APC/C activity by immunoprecipitating APC/C from CSF extracts at intervals after calcium addition using anti-Cdc27 antibodies (Kramer et al., 2000; Yu et al., 1996; Figure 3A). These immunoprecipitates were split into two aliquots, the first of which was analyzed by Western blotting with antibodies against Cdc27 and FZY, to determine whether the APC/C^{FZY} complex was intact. Because *Xenopus* eggs and early embryos do not contain the Cdh1 adaptor for APC/C, the APC/C^{FZY} complex is the only physiologically relevant form of an active APC/C in the egg extract system (Lorca et al., 1998). The second aliquot was added to a ubiquitination assay that also contained purified *Xenopus* E1 and E2 (Ubcx) enzymes, as well as a model APC/C substrate, ^{125}I-labeled *Xenopus* Cyclin B1 (amino acids 1–102; Yu et al., 1996).

The addition of calcium to a CSF extract containing sperm chromatin elicited a rapid wave of both FZY association to APC/C and APC/C ubiquitin ligase activity (Figure 3A). This wave of E3 enzyme activity corresponded closely to the timing of Cyclin B2 degradation in intact extracts (Figure 2A). By contrast, neither significant FZY association to APC/C nor increased Cyclin B1 ubiquitination were observed upon calcium addition to a CSF extract wherein the checkpoint had been activated by sperm chromatin and nocodazole. As a control, we analyzed the abundance of FZY in the soluble fraction of extracts after 5 min of stimulation with calcium (the input for anti-Cdc27 immunoprecipitations), and we found no difference in the amount of FZY in all cases (Figure 3B). To address the question of whether APC/C itself but not FZY is the target in the spindle checkpoint in *Xenopus* egg extracts, we added recombinant hFZY to APC/C complexes immunoprecipitated either from control extract or from extracts with activated checkpoint after 10 min of calcium addition. We performed an APC/C assay as above and found that hFZY activated APC/C from both extracts with indistinguishable efficiency (Figure 3C). We concluded that the spindle checkpoint in egg extract is mediated by sequestration of FZY from APC/C.

Remarkably, addition of RCC1 at moderate levels (5-fold endogenous) to extracts containing sperm chromatin and nocodazole restored the waves of both APC/C^{FZY} complex assembly and Cyclin B1 ubiquitination observed after calcium addition (Figure 3A). Consistent with our previous observations (Figure 2B), the peak of APC/C^{FZY} activation in the extract treated with this concentration of RCC1 occurred 5–10 min after the peak of control CSF extracts in which the checkpoint had never been activated (Figure 3A, compare right and left panels). These observations indicate that APC/C^{FZY} complex assembly is likely to be the key downstream target of RCC1-mediated checkpoint override.

Consistent with the fact that RCC1 does not elicit exit from CSF arrest prior to the addition of calcium (Figure 2), we did not observe an increased rate of Cyclin B1 ubiquitination without calcium addition (data not shown). These findings show that APC/C^{FZY} inhibition by CSF is insensitive to RCC1 levels, and demonstrate that the Ran pathway interacts specifically with the spindle checkpoint but not with other mechanisms of M phase arrest.

Ran-GTP Controls Loading of Checkpoint Proteins onto Kinetochores

Spindle checkpoint regulators accumulate on unattached kinetochores in close correlation with checkpoint activation (Millband and Hardwick, 2002), and we

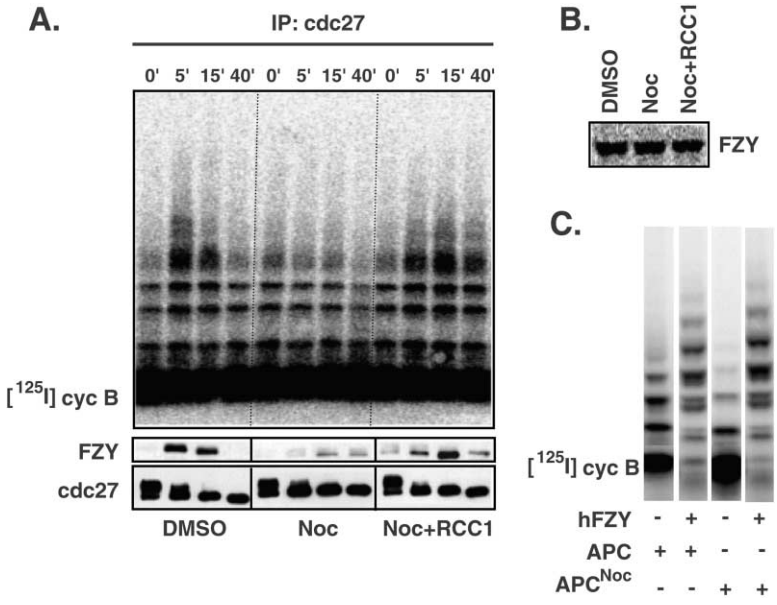

Figure 3. APC/C Activity Is Regulated by RCC1

(A) CSF extracts with nuclei and either DMSO (left), nocodazole (middle), or nocodazole plus 1.25 μM RCC1 (right) were incubated for 50 min at 24°C. After addition of 0.6 mM calcium, aliquots were removed at the indicated times and anti-Cdc27 antibody covalently bound to protein A-Sepharose beads was used to isolate APC/C complexes. One half of immunoprecipitates was processed for APC/C activity assays using iodinated destruction box of Cyclin B1 (see Experimental Procedures). Iodinated products of this reaction were analyzed by SDS-PAGE and autoradiography. The other half of the immunoprecipitate was assayed for the abundance of FZY and Cdc27 by Western blotting.

(B) The input of samples for immunoprecipitation corresponding to lanes 2, 6, and 10 in (A) was analyzed prior to immunoprecipitation by Western blotting with antibodies directed against FZY.

(C) APC/C was purified as in (A) from CSF extracts with nuclei and either DMSO (APC) or nocodazole (APC^{noc}) 10 min after the addition of calcium. Immunoprecipitates were analyzed for ubiquitination activity with or without addition of 100 ng of recombinant hFZY, as indicated.

tested whether this accumulation is sensitive to the concentration of RCC1. Kinetochores assembled on sperm chromatin in CSF extracts can be visualized as discrete foci by immunofluorescent staining with antibodies against centromeric proteins, such as CENP-A (McCleland et al., 2003; Figure 4A). As would be expected, Bub3 localized to chromosomal foci in nocodazole-treated CSF extracts that precisely correlated with CENP-A foci (Figure 4A, left column). RCC1 addition abolished Bub3-stained foci on chromosomes assembled in nocodazole-treated CSF extracts (Figure 4A, center column). Notably, RCC1 did not alter CENP-A staining in any detectable manner, suggesting that the underlying structure of the kinetochore had not been disrupted. We also examined the localization of Mad2, CENP-E, and Bub1 in CSF extracts containing nocodazole plus RCC1. In agreement with published results (Abrieu et al., 2000; Sharp-Baker and Chen, 2001), chromosomes incubated in CSF extracts treated with nocodazole showed very intense kinetochore-associated signals for Mad2 and CENP-E in comparison to chromosomes from control extracts lacking nocodazole (Figure 4B; note that these images show a single focal plane, so not all kinetochores are visible). As with Bub3, staining of foci with antibodies against Mad2, CENP-E, and Bub1 was essentially abolished through the addition of RCC1 protein. As indicated above, these extracts remained in M phase because CSF arrest is not compromised after RCC1 addition without calcium.

Similar to checkpoint override (Figure 2), we found that staining of checkpoint proteins on kinetochores was barely detectable with the addition of RCC1 at 10-fold endogenous concentrations; kinetochore association increased at intermediate concentrations from 10- to 1-fold over endogenous in a manner that was inversely proportional to the RCC1 levels (data not shown).

The majority of our experiments were conducted in the presence of nocodazole in order to distinguish between RCC1's role in assembly of checkpoint component on the kinetochore and its role in mitotic microtubule dynamics. However, we have performed a limited number of experiments in the absence of nocodazole, as spindles assembled around unreplicated chromosomes retain Bub1 protein at their kinetochores (Sharp-Baker and Chen, 2001; Tunquist et al., 2002; Figures 4B and 4C). Even under these circumstances, we observed that addition of RCC1 excludes Bub1 from the kinetochore, indicating that RCC1's effect is not restricted to the extreme case wherein all microtubules are depolymerized and microtubules' motor-dependent transport to kinetochores is eliminated. Notably, $RCC1^{D182}$ did not eliminate kinetochore association of any of the checkpoint proteins at any concentration tested (Figures 4A and 4B; data not shown).

In order to determine whether the localization of checkpoint proteins is directly responsive to Ran-GTP concentrations, we added recombinant RanGAP1 (5-fold endogenous) to the nocodazole-treated CSF extracts containing sperm chromatin and exogenous RCC1 (10-fold) protein (Figure 4B). We observed two patterns of behavior: Bub1 and Bub3 localized to kinetochore foci in extracts containing both RCC1 and RanGAP1, suggesting that they are directly responsive to Ran-GTP. By contrast, there was no observable increase in the chromosome-associated levels of CENP-E and Mad2 after RanGAP1 addition, suggesting that their binding sites could not be reestablished simply by lowering the concentration of Ran-GTP. These findings suggest not only that the association of checkpoint regulators to the mitotic kinetochore is sensitive to RCC1 levels, but also that there may be two pathways to detect alterations of RCC1 binding to chromatin, one of which

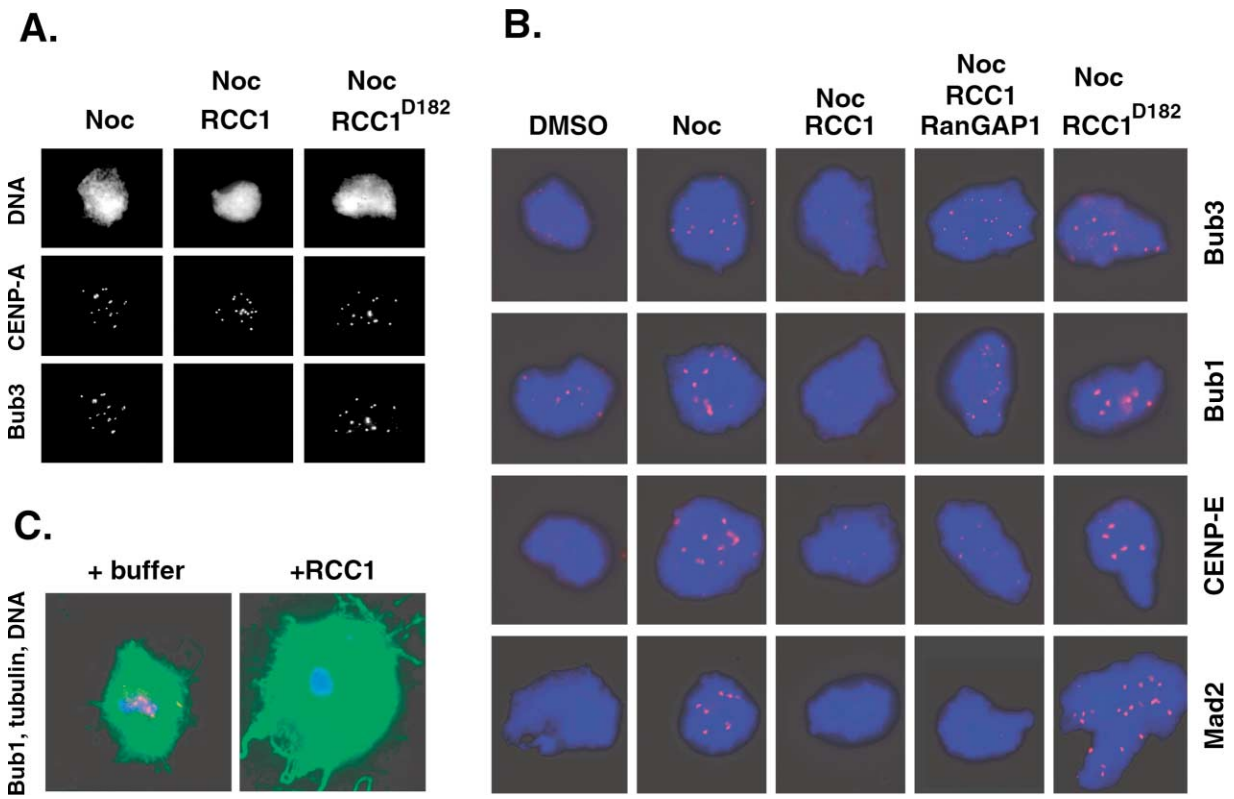

Figure 4. RCC1 Regulates Checkpoint Protein Loading onto Kinetochores

(A) CSF extracts with nuclei and nocodazole were incubated for 40 min at 24°C followed by addition of 2.5 μM RCC1 or 12.5 μM RCC1^{D182} for 20 min. Mitotic chromosomes were analyzed by indirect immunofluorescence with antibodies against CENP-A and Bub3 as indicated and stained with Hoechst 33342. Flattened stacks of images were taken for the same exposure and processed in the same manner.

(B) DMSO, nocodazole, 2.5 μM RCC1, 1.25 μM RanGAP1, and 12.5 μM RCC1^{D182} were added in the indicated combinations to CSF extracts with nuclei and incubated for 40 min at 24°C. Mitotic chromosomes were analyzed by indirect immunofluorescence with rabbit antibodies against Mad2, CENP-E, Bub1, or Bub3 as indicated and stained with Hoechst 33342. Single focal plane of images were taken for the same exposure time and processed in the same manner.

(C) Buffer or 2.5 μM RCC1 were added to CSF extracts containing 200 sperm/μl and rhodamine-labeled tubulin (shown in green). The reactions were incubated for 40 min at room temperature, fixed, and processed for immunofluorescent staining using antibodies directed against Bub1 (red).

may not rely strictly on Ran-GTP levels. Alternatively, there may be two classes of response to Ran-GTP levels, with Bub1 and Bub3 being able to bind kinetochores at higher local Ran-GTP concentrations than Mad2 and CENP-E.

Ran-GTP Controls Loading of Checkpoint Proteins onto Chromosomes

We examined purified chromosomes from nocodazole-treated CSF extracts with or without added RCC1, in order to determine whether there were gross changes in chromatin composition and to biochemically confirm changes in the levels of checkpoint proteins (Figure 5). First, we compared reactions containing a moderate level of wild-type RCC1 (7-fold endogenous) to a high concentration of the inactive RCC1^{D182} mutant (20-fold). After silver staining, chromosomal preparations from both reactions showed a complement of major chromatin proteins (e.g., core histones) that was indistinguishable from each other and from the control without added RCC1. Moreover, Western blotting analysis showed similar levels of phosphorylated histone H3 and Topoisomerase II in the three samples (Figure 5A). This observation suggests that RCC1 addition does not cause global changes in chromatin assembly or structure. By contrast, wild-type RCC1 caused a significant loss of Bub1, CENP-E, and Mad2 from the chromosomal fraction. Notably, we did not observe a similar decrease in the levels of Bub1, CENP-E, or Mad2 in the reaction with higher levels of RCC1^{D182}. In fact, chromosome-bound pools of these proteins frequently appeared to be elevated by the presence of RCC1^{D182}. This finding is completely consistent with the observation that RCC1^{D182} enhanced checkpoint arrest (Figure 2), apparently acting as an antagonist to the endogenous wild-type RCC1 protein. Second, we examined how the association of checkpoint proteins to chromatin varied as a function of RCC1 concentration. Similar to immunofluorescent staining of kinetochores (Figure 4 and data not shown), the amount of Bub3 protein associated with purified chromosomes from nocodazole-treated CSF extracts was inversely

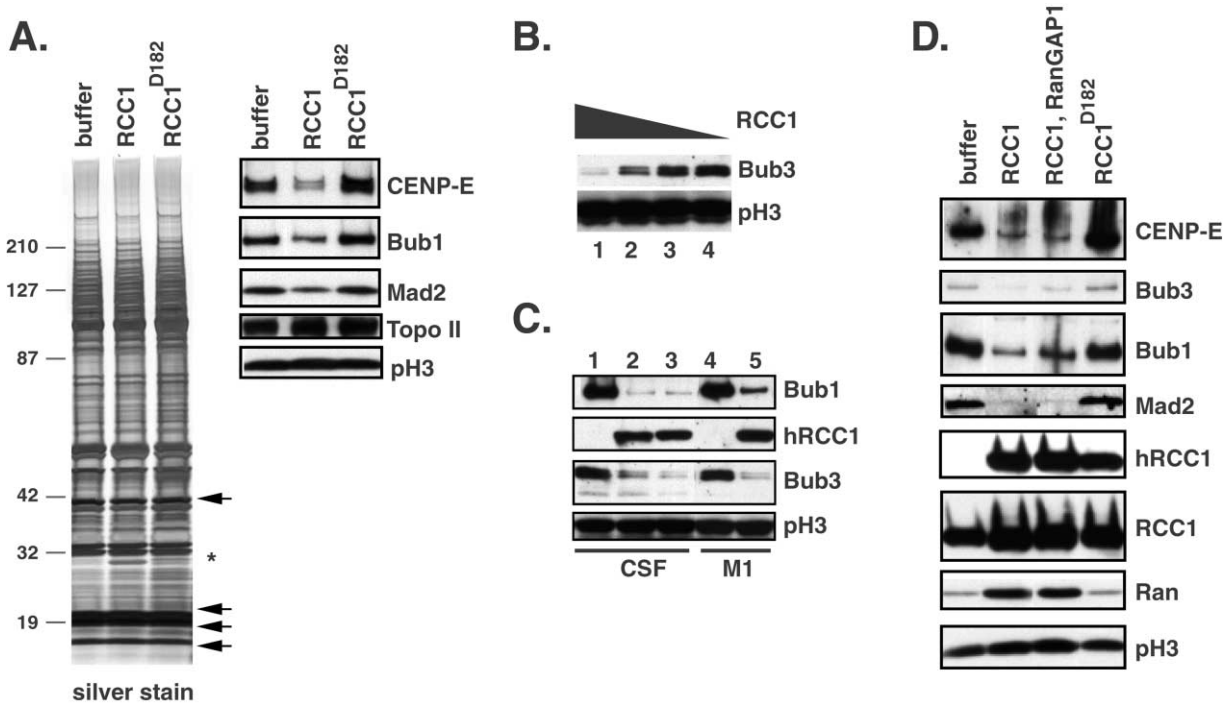

Figure 5. RCC1 Regulates Checkpoint Protein Loading onto Chromatin

(A) CSF extracts with nuclei and nocodazole were incubated either with buffer, with 1.75 μM RCC1, or with 5 μM RCC1^{D182} for 40 min at 24°C, as indicated. Mitotic chromosomes were purified and analyzed by SDS-PAGE and silver staining for the abundance of chromatin-associated proteins. Arrows indicate the positions of histones, and the asterisk shows the position of Ran. The same samples were analyzed by Western blotting for the presence of CENP-E, Bub1, Mad2, Topoisomerase II, and phosphorylated histone H3.

(B) CSF extracts with nuclei and nocodazole were incubated with increased concentrations of RCC1 (0.25 μM, 0.5 μM, 1 μM, and 2.5 μM; lanes 4 to 1, respectively) for 40 min at 24°C. Mitotic chromosomes were purified and analyzed by Western blotting for the presence of Bub3 and phosphorylated histone H3.

(C) CSF extracts with nuclei and nocodazole were supplemented with buffer (1) or with 2.5 μM RCC1 added either simultaneously with chromatin at t = 0 (2) or after incubation of extracts with chromatin for 40 min at 24°C followed by further incubation for 20 min with the protein (3). CSF extracts containing 5,000 sperm per μl were released into interphase. After 70 min, fresh CSF extract was added to drive interphase extracts into first mitosis. After nuclear envelope breakdown and chromatin condensation, nocodazole and buffer (4) or 2.5 μM RCC1 (5) were added for 25 min. Chromatin was purified and analyzed by Western blotting for the abundance of Bub1, Bub3, recombinant RCC1, and phosphorylated histone H3.

(D) Buffer, 2.5 μM RCC1, 2.5 μM RCC1 plus 1.25 μM RanGAP1, or 5 μM RCC1^{D182} were added to CSF extracts with nuclei and nocodazole and incubated for 50 min at 24°C. The chromatin fraction was analyzed by Western blotting for the presence of indicated proteins.

proportional to the amount of RCC1 added to the reaction in which the chromosomes were assembled (Figure 5B).

We examined whether the capacity of increased RCC1 levels to disrupt the spindle checkpoint after its activation (Figure 2C) might be a reflection of its ability to remove checkpoint regulators from assembled kinetochores. To do this, we analyzed chromatin preparations from nocodazole-treated CSF extracts by Western blotting (Figure 5C). Without the addition of RCC1, there was a significant amount of Bub1 and Bub3 bound to the chromosomes. Addition of RCC1 at the start of the reaction dramatically reduced the levels of Bub1 and Bub3, but did not significantly alter the level of phosphorylated histone H3 in these preparations. Notably, the levels of both Bub1 and Bub3 were also reduced when the RCC1 protein was added 40 min after the start of the reaction, when the kinetochores were fully assembled and the checkpoint signaling pathway had been activated (Figure 5C, lane 3).

Because the chromosomes in demembraned sperm nuclei preparations are unreplicated, we examined whether RCC1 could control the association of checkpoint proteins with replicated mitotic chromosomes (Figure 5C, lanes 4 and 5). To do this, we prepared chromatin from CSF extracts containing nuclei which were driven into interphase through the addition of calcium, allowed to form nuclei and replicate their DNA, and then driven back into mitosis with a fresh aliquot of CSF extract (Murray, 1991). After reestablishment of CSF arrest, as evidenced by nuclear envelope breakdown and chromosome condensation, nocodazole was added to the reactions with or without RCC1 protein. When chromatin from these reactions was subjected to Western blotting with antibodies against Bub1 and Bub3, both proteins were clearly associated with chromosomes in the reaction without supplemental RCC1. However, the levels of both Bub1 and Bub3 were dramatically reduced by RCC1 addition, although the level of phosphorylated histone H3 did not vary between the

preparations without and with RCC1. These observations clearly demonstrate that elevated levels of RCC1 are equally able to disrupt the assembly of checkpoint proteins on replicated and unreplicated kinetochores.

Finally, we investigated whether increased nucleotide hydrolysis on Ran-GTP could compensate for elevated levels of RCC1 (Figure 5D). Sperm chromosomes were added to CSF extracts with nocodazole and allowed to assemble in the presence of added RCC, RCC1^{D182}, or RCC1 plus RanGAP1. Chromatin preparations were made from these reactions, and assayed for the amount of associated checkpoint proteins by Western blotting. At higher levels of RCC1 (10-fold endogenous), we again saw substantial decreases in the levels of chromatin-associated CENP-E, Bub1, Bub3, and Mad2 relative to controls treated with nocodazole but not RCC1. Addition of RanGAP1 to RCC1-treated reactions caused moderate restoration of Bub1 and Bub3 levels on chromatin, but we saw no increase in the levels of Mad2 or CENP-E associated with chromatin in the same reactions (Figure 5D). These observations support both the conclusion that increased RCC1 concentrations can exclude checkpoint regulators from kinetochores, and that this exclusion is mediated by changes in Ran-GTP levels for at least some of these proteins.

Importin β Is Not Required for RCC1 Disruption of the Spindle Checkpoint

We were interested in whether Importin β may have a role in RCC1's inactivation of the spindle checkpoint, because it has been implicated in other mitotic roles of Ran. To address this question, we depleted over 95% of Importin β from CSF extracts using a fusion protein containing the Importin β binding domain of Importin α (Gorlich et al., 1996; Figure 6A). We added nocodazole to these depleted extracts, and assayed the association of checkpoint proteins to kinetochores, both by Western blotting of chromatin preparations (Figure 6B) and by immunofluorescence with anti-Bub3 antibodies (Figure 6C). We saw no significant difference between depleted and control extracts in the behavior of checkpoint proteins in either assay. Finally, we observed no difference in the capacity of RCC1 to override checkpoint arrest and promote cyclin B destruction and mitotic release after depletion of Importin β (Figure 6D). Taken together, these observations strongly suggest that Importin β is not an effector for Ran-GTP in regulating the association of checkpoint proteins to kinetochores.

RanBP2/RanGAP1 Depletion Disrupts Association of Checkpoint Proteins to Kinetochores

The experiments that we have shown above relied upon the addition of recombinant proteins to egg extracts. We wished to utilize an alternative approach to test the role of Ran in the spindle checkpoint by depleting Ran from CSF extracts using the Ran-GTP binding domain of Importin β (Nachury et al., 2001). We incubated His_6-tagged Importin β fusion protein (His-Impβ_{1-380}) that was covalently bound to Sepharose with extracts. We examined the depleted extract to determine the levels of Ran, Ran regulators, and checkpoint proteins by Western blotting (Figure 6A). The levels of RCC1, Importin β, all checkpoint proteins, and most pore proteins were unchanged by this procedure. Ran levels were decreased, but this depletion was incomplete, with roughly 40% of the endogenous protein remaining, presumably due to inability of His-Impβ_{1-380} to bind Ran-GDP. By contrast, RanGAP1 levels were dramatically decreased, to roughly 5% of the control level, and the RanBP1 and RanBP2 proteins were both eliminated. Therefore, treatment with His-Impβ_{1-380} produced extracts that possessed intact levels of RCC1 but that should have little or no capacity to hydrolyze Ran-GTP. Under these circumstances, Ran would be expected to accumulate in its GTP-bound form.

We incubated His-Impβ_{1-380}-treated CSF extracts with nocodazole and sperm chromatin, and stained chromosomes for components of the spindle checkpoint in order to determine whether the extracts retained the capacity to assemble checkpoint proteins into complexes on kinetochores. As shown for Bub1 (Figure 6B), checkpoint proteins bound to kinetochores in control extracts but not in the His-Impβ_{1-380}-treated samples. The absence of checkpoint components from chromosomes was also verified by Western blotting of chromosomal fractions (data not shown). Addition to such depleted extracts of Ran alone or Ran plus RanBP1 to control levels did not reestablish association of checkpoint proteins to kinetochores (Figure 6B). Notably, the restoration of RanGAP1 together with Ran and RanBP1 to control levels allowed measurable association of Bub1 to chromosomes, indicating that the elevation of Ran-GTP concentrations after RanGAP1 depletion causes the disruption of Bub1 binding. These findings utilize a completely distinct methodology for altering the relative rates of Ran nucleotide exchange and hydrolysis, and yet they fully support the conclusion from the earlier experiments that binding of Bub1 to kinetochores is directly responsive to Ran-GTP.

Discussion

RCC1 undergoes a radical redistribution onto chromosomes during mitosis in *Xenopus* egg extracts, closely coincident with the activation of the APC/C (Figure 1). In an effort to understand the meaning of the transient increase in RCC1 association to chromosomes, we have examined how addition of RCC1 alters mitotic progression in egg extracts. We found that moderate increases of RCC1 can relieve the spindle assembly checkpoint-mediated mitotic arrest. The capacity of RCC1 to reverse spindle checkpoint arrest appears to be quite specific, because other modes of M phase arrest (e.g., CSF arrest) are not compromised by increased levels of RCC1, and because we observe elimination of spindle checkpoint regulators away from kinetochores. Taken together, these results lead us to conclude that the Ran pathway is normally regulated in a highly dynamic manner during mitosis. These transitions of the Ran pathway can be mimicked by addition of exogenous RCC1 protein, triggering the metaphase-anaphase transition prematurely in the presence of unattached kinetochores. Our observations suggest that changes in RCC1's chromosomal

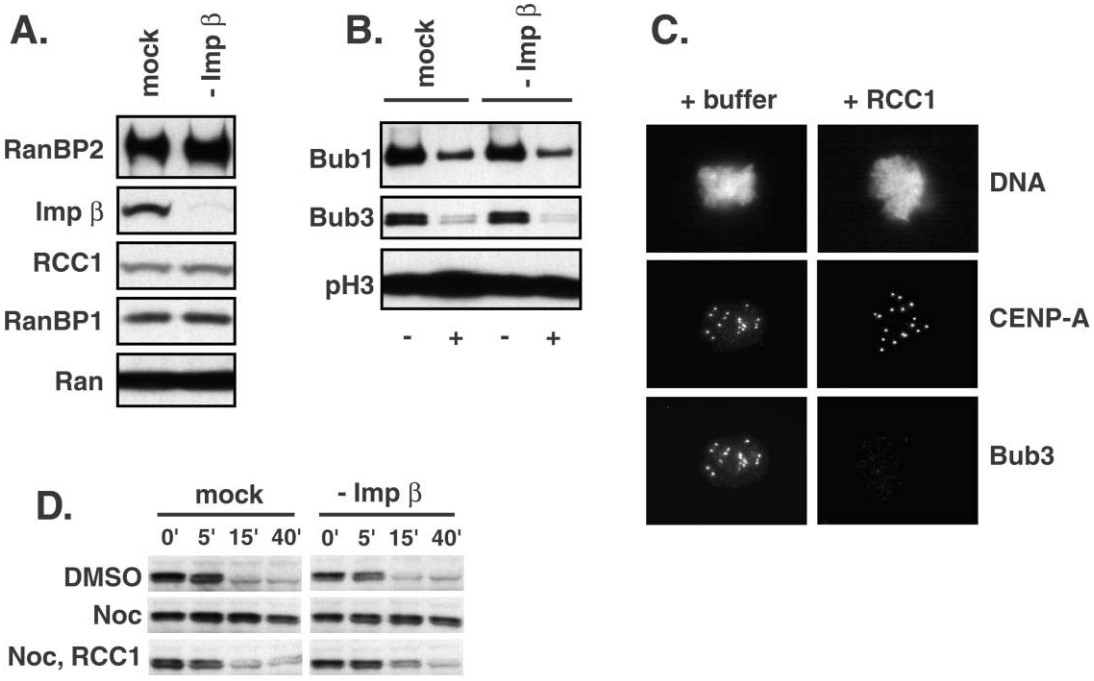

Figure 6. Importin β Is Dispensable for RanGTP-Regulated Kinetochore Localization of Checkpoint Proteins

(A) CSF extract after mock or Importin β depletion were tested for the abundance of RanBP2, RanBP1, RCC1, Ran, and Importin β.

(B) Mock- or Importin β-depleted CSF extracts were incubated with nuclei and nocodazole for 30 min at 23°C followed by addition of 2.5 μM RCC1 for 20 min. Chromatin was purified and analyzed for the abundance of Bub1, Bub3, and phosphorylated H3.

(C) Importin β-depleted CSF extract was incubated with sperm nuclei and nocodazole for 40 min at 23°C followed by addition of 2.5 μM RCC1 for 20 min. Chromatin was processed as in Figure 4A for staining of Bub3 and CENP-A.

(D) Extracts as in (B) were tested for the ability to maintain checkpoint after addition of calcium for the indicated times. Cyclin B abundance was estimated as above. Samples from mock-treated extracts are shown in the left panels, and samples from Importin β-depleted extracts are shown in the right panels.

dynamics may be a key link in the chain of events between completion of metaphase spindle assembly and mitotic exit.

The Spindle Checkpoint in *Xenopus* Egg Extracts

It was recently demonstrated that FZY in HeLa cells associates with BubR1, Mad2, and Bub3 in a complex that has been named the MCC (mitotic checkpoint complex; Sudakin et al., 2001). This finding led to the proposal that the MCC is a physiologically relevant inhibitor of mitotic APC/C, and that unattached kinetochores inhibit cell cycle progression by preventing inactivation of the relatively labile MCC complex. By contrast to the observations from HeLa cells, we find APC/C does not associate with FZY under checkpoint conditions in egg extracts (Figure 3), arguing against the formation of a stable MCC-APC/C complex. Recombinant human FZY protein was equally able to activate APC/C from extracts in which the checkpoint was or was not established (Figure 3C), suggesting that the failure of FZY protein to bind APC/C may result from a modification of the FZY protein and/or its association to other proteins in response to kinetochores that are unattached or inappropriately attached. Increased levels of RCC1 were able to reverse the block preventing APC/C association with FZY, clearly indicating that FZY activation lies downstream of RCC1 in this APC/C activation pathway, and that it is likely to be the key downstream target of RCC1-mediated checkpoint override.

RCC1 Acts at the Kinetochore to Disrupt the Spindle Checkpoint

We examined the capacity of RCC1 to disrupt the origination of the checkpoint signal, particularly the binding of spindle checkpoint components to the kinetochore. Increased levels of RCC1 released Bub1, Bub3, Mad2, and CENP-E from kinetochores in CSF extracts containing nocodazole (Figures 4 and 5). While it remains possible that RCC1 might also influence other parts of the checkpoint signaling pathway, we strongly favor the idea that elevated levels of RCC1 caused mitotic exit primarily by releasing checkpoint regulators from kinetochores, as disruption of these interactions should be sufficient to inactivate the checkpoint and allow mitotic exit. Furthermore, we observed a close correspondence between RCC1's capacity to cause displacement of checkpoint proteins from kinetochores and its capacity to alleviate checkpoint arrest. The concentrations of RCC1 required to dissociate checkpoint proteins from the kinetochores (Figure 5B) corresponded closely to

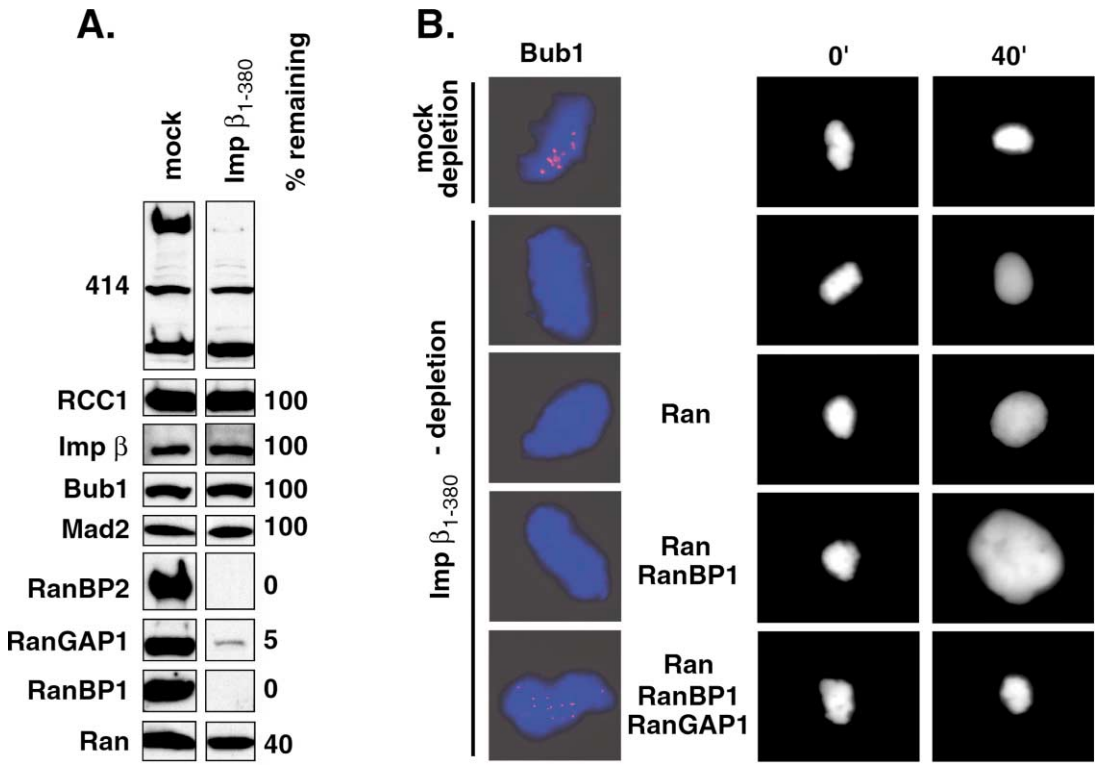

Figure 7. Depletion of RanGAP1 from Egg Extract Inactivates the Spindle Checkpoint

(A) CSF extracts were incubated either with Sepharose (mock) or Sepharose that had been covalently coupled to the Ran binding domain of Importin β (Impβ$_{1–380}$). After removal of the beads and associated proteins, the supernatants from each incubation were analyzed by Western blotting with antibodies against the indicated proteins.

(B) Nuclei and nocodazole were added to mock-depleted extracts, Impβ$_{1–380}$-depleted extracts, or Impβ$_{1–380}$-depleted extracts supplemented with Ran, RanBP1, and RanGAP1 (to endogenous levels) in the indicated combinations. After incubation for 40 min at 23°C, the reactions were divided in two. One half was evaluated by immunofluorescence for Bub1 association to kinetochores. Calcium was added to the other half. The stability of the spindle checkpoint was evaluated by examining DNA morphology using Hoechst 33342 staining of chromosomes at calcium addition (0′) and with a further 40 min incubation (40′).

those required to promote mitotic release of nocodazole-treated CSF extracts after calcium addition (Figure 2B). Notably, RCC1 could promote both of these events even when it was added after the kinetochore had been assembled and the checkpoint pathway had been activated (Figures 2C and 5C).

Importin β has previously been implicated as the primary effector for Ran in spindle assembly (Dasso, 2002). However, Importin β does not appear to have a significant role as an effector for spindle checkpoint release (Figure 6). It remains possible that another transport receptor may fulfill this role (Macara, 2001). Reports showing the localization of nuclear pore proteins to the kinetochore (Belgareh et al., 2001; Joseph et al., 2002) also offer the interesting possibility that nuclear pore components might act as Ran effectors in checkpoint control. This possibility is particularly intriguing in light of the fact that checkpoint regulators also associate with nuclear pores during interphase (Campbell et al., 2001; Iouk et al., 2002).

The Interaction of RCC1 with Mitotic Chromatin

The amount of RCC1 on chromatin increased dramatically at the onset of anaphase (Figure 1). In typical experiments, this increase results in a 7- to 10-fold elevation in the level of RCC1 on the mitotic chromosomes over the amount of RCC1 found on interphase chromatin. The 5- to 7-fold elevation of RCC1 concentration required to override checkpoint arrest probably reflects the levels of exogenous RCC1 required to mimic the wave of RCC1 binding to chromatin immediately prior to anaphase. Because RCC1 is a chromatin binding protein, there is naturally a concern as to whether increased levels of RCC1 may disrupt the spindle checkpoint by interfering with kinetochores in a nonspecific manner. There are several reasons to believe that this is not the case. First, the resident centromeric protein CENP-A was correctly assembled on kinetochores after RCC1 addition (Figures 4 and 6). Second, RCC1 was able to disrupt the checkpoint even after the assembly of kinetochores on sperm chromatin and the activation of the checkpoint pathway (Figure 2). Third, there were no changes of chromosome morphology or composition of major chromatin proteins (Figure 5) at the concentrations of RCC1 required for checkpoint override. Fourth, RanGAP1 and RanBP1 could reestablish checkpoint arrest, although these proteins did not alter the interactions of RCC1 with chromatin (Figures 2 and 5). Rather, their capacity to reverse the effects of RCC1 argues that the checkpoint is sensitive to the overall levels of Ran-GTP. Finally,

depletion of extracts with Impβ_{1-380} abrogated checkpoint arrest and Bub1 binding to kinetochores without altering the levels of RCC1 associated with chromatin (Figure 7 and data not shown).

Ran in Mitosis

We would like to propose a simple scheme that would both account for cell cycle regulation of RCC1's association to chromatin and for the capacity of exogenous RCC1 to override spindle checkpoint arrest (see Supplemental Figure S1 at http://www.developmentalcell.com/cgi/content/full/5/1/99/DC1). During prophase, unattached kinetochores intensely activate the spindle checkpoint, which is reflected by the accumulation of checkpoint regulators at the kinetochores. After microtubule attachment, the checkpoint regulators are still required for preventing any premature transition into anaphase prior to chromosome alignment, but these signals may be generated at a lower level, such that only Bub1 can still be stably visualized at the kinetochore, while the interaction of Mad2 has become too short lived to observe (Shannon et al., 2002). Complete chromosome alignment on the metaphase plate coincides with or triggers the increased binding of RCC1 to chromosomes, resulting in the local elevation of Ran-GTP levels and the ejection of the final population of kinetochore-associated Bub1 protein. This final step coincides with the onset of anaphase. Notably, RanGAP1 and RanBP2 are localized to kinetochores of metaphase chromosomes in HeLa cells, but their kinetochore localization is lost after treatment of cells with nocodazole (Joseph et al., 2002). We have similarly found that RanGAP1 and RanBP2 are absent from mitotic chromosomes in nocodazole-treated egg extracts (data not shown). We would not expect that relocalization of RanGAP1 and RanBP2 played a major role in the findings presented in this report, because these experiments were largely conducted in the presence of nocodazole. However, it is possible that the redistribution of these proteins plays an important role in coupling the Ran pathway to spindle assembly or checkpoint controls in vivo.

We would further speculate that the capacity of Ran-GTP to dissociate checkpoint proteins from kinetochores might play a separate important role during interphase. Soon after nuclear envelope formation, the nucleus and cytosol develop a polarized distribution of Ran-GTP due to the restriction of Ran-GDP nucleotide exchange to the nucleus and Ran-GTP nucleotide hydrolysis to the cytoplasm (Macara, 2001). The sequestration of chromosomes to the high-Ran-GTP environment of the nucleus could assure that kinetochores are fully disassembled after mitosis and that spindle checkpoint proteins do not inappropriately associate with centromeres during interphase.

Experimental Procedures

Recombinant Protein Expression, Cloning, and Antibodies

Untagged human RCC1, RCC1^{D182} (Azuma et al., 1996), untagged human RanGAP1 (Haberland and Gerke, 1999), untagged *Xenopus* Ran (Dasso et al., 1994), RanBP1 (Kalab et al., 1999), and Ubcx (Yu et al., 1996) were expressed in *E. coli* as described. The ubiquitin E1 enzyme was purified with ubiquitin-Sepharose using a protocol that was otherwise as described for the SUMO-1 E1 enzyme (Desterro et al., 1999). The expression of untagged RanBP1 from a pET3a vector was induced in *E. coli*. Bacteria were lysed in B-PER buffer (Pierce) and RanBP1 was purified by FPLC using Q-Sepharose and Sephacryl S100. The Cyclin B1 destruction box fragment (Yu et al., 1996) was expressed in pET28 vector, purified on Ni-NTA beads followed by chromatography on Mono Q and Mono S columns, and labeled with ^{125}I using the chloramine T procedure. The IBB domain of Importin α (Gorlich et al., 1996) was amplified by PCR, and cloned into Nco1/Nde1-cut pET28a that contains zz-tag inserted in Nde1/Xho1. The Ran-GTP binding fragment of *Xenopus* Importin β (amino acids 1–380) was amplified by PCR, and cloned into the Nde1/BamH1 sites of pET28a vector. The *Xenopus* Securin full-length cDNA was amplified from a *Xenopus* cDNA library, and cloned into Nde1/Xho1-cut pET30a. Securin protein was expressed in the reticulocyte lysate (TnT Quick, Promega) in the presence of ^{35}S and added to egg extract. The *Xenopus* FZY/Cdc20 full-length cDNA was amplified by PCR from a *Xenopus* cDNA library, and cloned into Nde1/BamH1-cut pET23a. The protein was expressed and purified as described (Kotani et al., 1999). Baculovirus-expressed FZY/Cdc20 was purified as described (Kramer et al., 2000). All proteins were dialyzed against PBS except for RanGAP1, which was dialyzed against XBG buffer (10 mM HEPES-KOH [pH 7.7], 100 mM KCl, 2 mM $MgCl_2$, 0.1 mM $CaCl_2$, 50 mM sucrose, and 5% glycerol).

Antibodies against the following proteins were used: *Xenopus* RCC1, RanBP1, RanBP2 (Saitoh et al., 1996), human RCC1 (clone 3D11, MBL), Ran, Cdc27, Importin β (Transduction Laboratories), *Xenopus* Cyclin B2 (kindly provided by T. Hunt), phosphorylated H3 (Upstate Biotechnology), *Xenopus* CENP-E (kindly provided by D. Cleveland), *Xenopus* Bub1, Bub3, Mad2 (kindly provided by J.L. Maller and R.H. Chen), Topoisomerase II (DNATop2AB, RDI), phosphorylated ERK1/2 (Cell Signaling), *Xenopus* CENP-A (kindly provided by T. Stukenberg), FG-containing nucleoporins (mAb414, Babco). Goat anti-rabbit and goat anti-chicken antibodies coupled to Alexa Fluor 594 and 488 were from Molecular Probes. Antibodies against recombinant *Xenopus* FZY were raised in rabbits and affinity purified.

Extracts

Low-speed extracts of *Xenopus* eggs arrested by CSF and cycling extracts were prepared as described (Murray, 1991). Where indicated, Texas red-labeled tubulin was added to a final concentration of 0.1 mg/ml. Where necessary, reactions were fixed and spun onto coverslips as described (Desai et al., 1999). Unless otherwise specified, all reactions contained 10,000 sperm nuclei per μl.

Preparation of Importin β- and RanBP2/RanGAP1/RanBP1-Depleted Extracts

CNBr-Sepharose or IgG-Sepharose beads (0.4 ml) were coupled to 5 mg of Impβ_{1-380} and 2 mg of IBB domain (Gorlich et al., 1996), respectively. The beads were blocked with 5% milk for 30 min at room temperature, washed with CSF-XB buffer, and incubated with 1.2 ml of CSF extract for 15 min at 24°C followed by 40 min at 4°C with rotation. The beads were removed by pelleting. Mock-depleted extracts were treated identically but with addition of noncoupled Sepharose.

Immunofluorescence and Chromatin Purification

For purification of chromatin in experiments with CSF or cycling extracts, 50 μl of each reaction was diluted ten times with buffer B (10 mM HEPES-KOH [pH 7.7], 50 mM KCl, 2 mM $MgCl_2$, 5 mM EGTA, and 40 mM β-glycerophosphate) containing leupeptin, pepstatin, aprotinin (10 μg/ml each), and 15% glycerol, and incubated for 1 min at room temperature. Extracts were then layered onto 40% glycerol cushion in buffer B and immediately centrifuged for 5 min at 4°C at 20,000 $\times$ g. The pellet was resuspended in buffer B containing 1% Triton X-100, and the centrifugation step was repeated. The resulting pellet was boiled in 50 μl SDS-PAGE sample buffer.

For immunofluorescence, 20 μl of each reaction was diluted 15-fold with buffer B containing 25% glycerol and 1% Triton X-100, and then mixed with 600 μl fixation buffer (buffer B, containing 25% glycerol and 6% formaldehyde) for 10 min at room temperature prior to layering onto 45% glycerol cushion in buffer B. Chromatin and

spindles were pelleted onto coverslips for 15 min at 8°C at 6500 × g and postfixed with −20°C methanol. CENP-A and Bub3 in Figures 4A and 6C were stained as described (McCleland et al., 2003).

APC/C Assay

One hundred microliters of extracts at the indicated time points were frozen in liquid nitrogen. The samples were thawed and diluted 10-fold with buffer B containing 50 mM sucrose, leupeptin, pepstatin, and aprotinin (10 μg/ml each), 100 nM okadaic acid, and 1 mM DTT. The diluted mixture was centrifuged for 20 min at 16,000 × g at 4°C. The supernatant was mixed with 10 μl protein A beads covalently bound to Cdc27 antibody and incubated for 2 hr at 4°C. The beads were pelleted and washed four times with buffer B containing 1% Triton X-100 and once with buffer B. The ubiquitination reaction was performed for 40 min at 24°C in 13 μl of buffer B containing ATP regeneration mixture, 1 mg/ml ubiquitin (Sigma), 10 μg/ml *Xenopus* E1, 50 μg/ml Ubcx, and 50–150 ng iodinated Cyclin B1. One hundred nanograms of baculovirus-expressed purified FZY/Cdc20 was added to reactions where indicated. Reactions were boiled in sample buffer and ubiquitination activity was quantified with the ImageQuant version 3 program from Molecular Dynamics. The amount of FZY associated with APC/C was analyzed by Western blotting.

Acknowledgments

We would like to thank T. Hunt, D. Cleveland, R. Chen, J. Maller, V. Gerke, T. Nishimoto, T. Stukenberg, M. Kirschner, and H. Yu for providing us with reagents. We are also very grateful to Y. Azuma for helpful comments and fruitful discussion during the work, J. Joseph for help with preparation of RanGAP1, and B.B. Quimby for critical comments on the manuscript.

Received: December 17, 2002
Revised: April 14, 2003
Accepted: April 18, 2003
Published: July 7, 2003

References

Abrieu, A., Kahana, J.A., Wood, K.W., and Cleveland, D.W. (2000). CENP-E as an essential component of the mitotic checkpoint in vitro. Cell *102*, 817–826.

Azuma, Y., Seino, H., Seki, T., Uzawa, S., Klebe, C., Ohba, T., Wittinghofer, A., Hayashi, N., and Nishimoto, T. (1996). Conserved histidine residues of RCC1 are essential for nucleotide exchange on Ran. J. Biochem. (Tokyo) *120*, 82–91.

Belgareh, N., Rabut, G., Bai, S.W., van Overbeek, M., Beaudouin, J., Daigle, N., Zatsepina, O.V., Pasteau, F., Labas, V., Fromont-Racine, M., et al. (2001). An evolutionarily conserved NPC subcomplex, which redistributes in part to kinetochores in mammalian cells. J. Cell Biol. *154*, 1147–1160.

Bischoff, F.R., Krebber, H., Smirnova, E., Dong, W., and Ponstingl, H. (1995). Co-activation of RanGTPase and inhibition of GTP dissociation by Ran-GTP binding protein RanBP1. EMBO J. *14*, 705–715.

Campbell, M.S., Chan, G.K., and Yen, T.J. (2001). Mitotic checkpoint proteins HsMAD1 and HsMAD2 are associated with nuclear pore complexes in interphase. J. Cell Sci. *114*, 953–963.

Chen, R.H., and Murray, A. (1997). Characterization of spindle assembly checkpoint in *Xenopus* egg extracts. Methods Enzymol. *283*, 572–584.

Chen, R.H., Waters, J.C., Salmon, E.D., and Murray, A.W. (1996). Association of spindle assembly checkpoint component XMAD2 with unattached kinetochores. Science *274*, 242–246.

Dasso, M. (2002). The Ran GTPase: theme and variations. Curr. Biol. *12*, R502–R508.

Dasso, M., Seki, T., Azuma, Y., Ohba, T., and Nishimoto, T. (1994). A mutant form of the Ran/TC4 protein disrupts nuclear function in *Xenopus laevis* egg extracts by inhibiting the RCC1 protein, a regulator of chromosome condensation. EMBO J. *13*, 5732–5744.

Desai, A., Murray, A., Mitchison, T.J., and Walczak, C.E. (1999). The use of *Xenopus* egg extracts to study mitotic spindle assembly and function in vitro. Methods Cell Biol. *61*, 385–412.

Desterro, J.M., Rodriguez, M.S., Kemp, G.D., and Hay, R.T. (1999). Identification of the enzyme required for activation of the small ubiquitin-like protein SUMO-1. J. Biol. Chem. *274*, 10618–10624.

Gorlich, D., Henklein, P., Laskey, R.A., and Hartmann, E. (1996). A 41 amino acid motif in importin-α confers binding to importin-β and hence transit into the nucleus. EMBO J. *15*, 1810–1817.

Haberland, J., and Gerke, V. (1999). Conserved charged residues in the leucine-rich repeat domain of the Ran GTPase activating protein are required for Ran binding and GTPase activation. Biochem. J. *343*, 653–662.

Iouk, T., Kerscher, O., Scott, R.J., Basrai, M.A., and Wozniak, R.W. (2002). The yeast nuclear pore complex functionally interacts with components of the spindle assembly checkpoint. J. Cell Biol. *159*, 807–819.

Joseph, J., Tan, S.H., Karpova, T.S., McNally, J.G., and Dasso, M. (2002). SUMO-1 targets RanGAP1 to kinetochores and mitotic spindles. J. Cell Biol. *156*, 595–602.

Kalab, P., Pu, R.T., and Dasso, M. (1999). The ran GTPase regulates mitotic spindle assembly. Curr. Biol. *9*, 481–484.

Kalab, P., Weis, K., and Heald, R. (2002). Visualization of a Ran-GTP gradient in interphase and mitotic *Xenopus* egg extracts. Science *295*, 2452–2456.

Kotani, S., Tanaka, H., Yasuda, H., and Todokoro, K. (1999). Regulation of APC activity by phosphorylation and regulatory factors. J. Cell Biol. *146*, 791–800.

Kramer, E.R., Scheuringer, N., Podtelejnikov, A.V., Mann, M., and Peters, J.M. (2000). Mitotic regulation of the APC activator proteins CDC20 and CDH1. Mol. Biol. Cell *11*, 1555–1569.

Lorca, T., Castro, A., Martinez, A.M., Vigneron, S., Morin, N., Sigrist, S., Lehner, C., Doree, M., and Labbe, J.C. (1998). Fizzy is required for activation of the APC/cyclosome in *Xenopus* egg extracts. EMBO J. *17*, 3565–3575.

Macara, I.G. (2001). Transport into and out of the nucleus. Microbiol. Mol. Biol. Rev. *65*, 570–594.

McCleland, M.L., Gardner, R.D., Kallio, M.J., Daum, J.R., Gorbsky, G.J., Burke, D.J., and Stukenberg, P.T. (2003). The highly conserved Ndc80 complex is required for kinetochore assembly, chromosome congression, and spindle checkpoint activity. Genes Dev. *17*, 101–114.

Millband, D.N., and Hardwick, K.G. (2002). Fission yeast Mad3p is required for Mad2p to inhibit the anaphase-promoting complex and localizes to kinetochores in a Bub1p-, Bub3p-, and Mph1p-dependent manner. Mol. Cell. Biol. *22*, 2728–2742.

Murray, A.W. (1991). Cell cycle extracts. Methods Cell Biol. *36*, 581–605.

Musacchio, A., and Hardwick, K.G. (2002). The spindle checkpoint: structural insights into dynamic signalling. Nat. Rev. Mol. Cell. Biol. *3*, 731–741.

Nachury, M.V., Maresca, T.J., Salmon, W.C., Waterman-Storer, C.M., Heald, R., and Weis, K. (2001). Importin β is a mitotic target of the small GTPase Ran in spindle assembly. Cell *104*, 95–106.

Peters, J.M. (2002). The anaphase-promoting complex: proteolysis in mitosis and beyond. Mol. Cell *9*, 931–943.

Pu, R.T., and Dasso, M. (1997). The balance of RanBP1 and RCC1 is critical for nuclear assembly and nuclear transport. Mol. Biol. Cell *8*, 1955–1970.

Saitoh, H., Cooke, C.A., Burgess, W.H., Earnshaw, W.C., and Dasso, M. (1996). Direct and indirect association of the small GTPase ran with nuclear pore proteins and soluble transport factors: studies in *Xenopus laevis* egg extracts. Mol. Biol. Cell *7*, 1319–1334.

Sazer, S., and Dasso, M. (2000). The ran decathlon: multiple roles of Ran. J. Cell Sci. *113*, 1111–1118.

Shannon, K.B., Canman, J.C., and Salmon, E.D. (2002). Mad2 and BubR1 function in a single checkpoint pathway that responds to a loss of tension. Mol. Biol. Cell *13*, 3706–3719.

Sharp-Baker, H., and Chen, R.H. (2001). Spindle checkpoint protein

Bub1 is required for kinetochore localization of Mad1, Mad2, Bub3, and CENP-E, independently of its kinase activity. J. Cell Biol. *153*, 1239–1250.

Sudakin, V., Chan, G.K., and Yen, T.J. (2001). Checkpoint inhibition of the APC/C in HeLa cells is mediated by a complex of BUBR1, BUB3, CDC20, and MAD2. J. Cell Biol. *154*, 925–936.

Tunquist, B.J., Schwab, M.S., Chen, L.G., and Maller, J.L. (2002). The spindle checkpoint kinase bub1 and cyclin e/cdk2 both contribute to the establishment of meiotic metaphase arrest by cytostatic factor. Curr. Biol. *12*, 1027–1033.

Yu, H., King, R.W., Peters, J.M., and Kirschner, M.W. (1996). Identification of a novel ubiquitin-conjugating enzyme involved in mitotic cyclin degradation. Curr. Biol. *6*, 455–466.